Arabian Journal of Chemistry (2022) **15**, 104033

King Saud University

Arabian Journal of Chemistry

www.ksu.edu.sa
www.sciencedirect.com

ORIGINAL ARTICLE

In silico and *in vivo* study of adulticidal activity from *Ayapana triplinervis* essential oils nano-emulsion against *Aedes aegypti*

Alex Bruno Lobato Rodrigues [a,*], Rosany Lopes Martins [a], Érica de Menezes Rabelo [a], Jonathan Lopes de Matos [a], Lizandra Lima Santos [b], Lethicia Barreto Brandão [b], Renata do Socorro Barbosa Chaves [b], Anderson Luiz Pena da Costa [b], Cleidjane Gomes Faustino [b], Dayse Maria da Cunha Sá [b], Ana Luzia Ferreira Farias [b], Patrick de Castrio Cantuaria [a], Sheylla Susan Moreira da Silva de Almeida [a,b]

[a] *Postgraduate Program in Biodiversity and Biotechnology -Network BIONORTE, Laboratory of Pharmacognosy and Phytochemistry, Federal University of Amapá, Highway Juscelino Kubistichek, Km 02, 68.902-280, Macapá, Brazil*
[b] *Postgraduate Program of Pharmaceutical Innovation, Laboratory of Pharmacognosy and Phytochemistry, Federal University of Amapá, Highway Juscelino Kubistichek, Km 02, 68.902-280, Macapá, Brazil*

Received 30 July 2021; accepted 5 June 2022
Available online 11 June 2022

KEYWORDS

Nanoinsecticide;
Molecular docking;
Natural products;
Nanobiotechnology

Abstract Nanoinsecticides of plant origin have advantages in the resistance of *Aedes aegypti*, vectors of infectious diseases. The objective of this study was to evaluate the insecticidal potential of *Ayapana triplinervis* essential oil nano-emulsions using *in silico* and *in vivo* assays in an *Aedes aegypti* model. Molecular docking showed that minority compounds present in the morphotype A essential oil have a more significant binding affinity to inhibit acetylcholinesterase and juvenile hormone receptors. Aedes aegypti adults were susceptible to A. triplinervis at 150 µg.mL-1 in a diagnostic time of 15 min for morphotype A essential oil nano-emulsion and 45 min for morphotype B essential oil nano-emulsion. The evaluation of toxicity in Swiss albino mice indicated that the nano-emulsions had low acute dermal toxicity and presented LD_{50} greater than 2000 mg.

* Corresponding author.
E-mail addresses: alexrodrigues.quim@gmail.com, alex.rodrigues@unifap.br (Alex Bruno Lobato Rodrigues).
Peer review under responsibility of King Saud University.

Production and hosting by Elsevier

https://doi.org/10.1016/j.arabjc.2022.104033
1878-5352 Published by Elsevier B.V. on behalf of King Saud University.

Kg^{-1}. Thus, it is possible to conclude that nano-emulsions have the potential to be used in the chemical control of *A. aegypti*.

1. Introduction

The mosquito *Aedes aegypti* is the vector of arboviruses such as dengue (DENGV), zika (ZICV), and chikungunya (CHIKV) and represents a major public health problem. The culicide can infect with a single virus type or with double and even triple co-infections of DENGV, ZICV, and CHIKV. There are no vaccines capable of controlling *A. aegypti* transmitted diseases, so vector control with synthetic insecticides is a key strategy for the management of related epidemics (Rückert et al., 2017).

However, a genetic mutation was detected in the region that decodes the sodium and potassium channel in resistant *A. aegypti* strains from Brazil. This is done by replacing a valine with leucine and phenylalanine with a cysteine, reducing the mosquitoes' susceptibility to pyrethroid, an important class of insecticides recommended by the World Health Organization (WHO) for chemical vector control (Haddi et al., 2017). In this context, plants have become an alternative in the search for bioactive substances with diverse chemical structures and new mechanisms of action for the control of *A. aegypti* (Brandão et al., 2021; Chaves et al., 2020).

The Asteraceae family has drawn attention to their ethnobotanical and ethnopharmacological employment in traditional communities. However, the phylogenetic, taxonomic, and chemosystematic information is incipient, reflecting the presence of the little-known genus (Gustafsson and Bremer, 1995).

Among the species of medicinal interest in the Asteraceae family, the *Ayapana triplinervis* (VAHL) R. M. King & H. Rob can be highlighted. This species is found in Brazil, Ecuador, Peru, Puerto Rico, and Guianas, besides having adapted in other countries such as India and Vietnam (Gauvin-Bialecki and Marodon, 2008). *A. triplinervis* can be found in two types: morphotype A, popularly called "japana-branca", and morphotype B, which is known as "japana-roxa"(Nery et al., 2014).

Phytochemically, the methanolic extract of *A. triplinervis* leaves has a predominance of hexadecanoic acid, tetradecacetic acid, and octadecanoic acid, with proven hypocholestatic, antioxidant, antiproliferative, and anticancer bioactivity (Selvamangai and Bhaskar, 2012). In another study, the methanolic extract showed the inhibition of 59% of melanomas using low cytotoxicity (Arung et al., 2012). The hydroalcoholic extract confirmed the anxiolytic, sedative, and behavioral antidepressant effects in the central nervous system in several animal models (Melo et al., 2013).

The crude ethanolic, methanolic, and petroleum ether extract had antimicrobial activity against different bacteria such as *S. epidermis*, *E. coli*, *S. typhi*, *V. parahaemolytcus*, *E. faecalis*, *S. aureus*, *S. epidermidis*, *M. leuteus*, *P. aeruginosa*, *V. cholera*, and against fungi *A. niger*, *A. flavus*, *A. solani* and *F. solani* in different concentrations.

Despite their significant potential for chemical control of vectors of infectious diseases, the essential oils of *A. triplinervis* morphotypes are susceptible to volatility and oxidation using oxygen and light, affecting the biological activity of their constituents. One way to enable protection against degradation and oxidation of essential oils is through the development of a technological nanoemulsification system, which offers advantages such as ease of handling, stability, protection against oxidation, better distribution, and controlled release (Wu et al., 2015).

Some studies using nano-emulsions as biocides have received prominence in the scientific literature, either by decreasing the lethal concentration of the product or by enabling a delivery and bioavailability mechanism in a polar environment. Nano-emulsions containing essential oils of *Ageratum conyzoides*, *Achillea fragantissima,* and *Tagetes minuta* and had a particle size less than or equal to 136 nm with high insecticidal activity against *Callosobruchus maculatus* with $LC_{50} < 40.5\ \mu l.L^{-1}$ (Nenaah et al., 2015). Nano-emulsions of *Cymbopogon citratus* essential oil with a hydrodynamic diameter equal to 11 nm and high biocide activity in *E. coli* (Guerra-Rosas et al., 2016). Thyme nano-emulsion with a particle diameter of 150 nm showed MIC 200 $\mu g.mL^{-1}$ in the control of the yeast *Zygosaccharomyces bailii*, demonstrating the biocide potential of nanostructured systems (Chang et al., 2015).

The potential for inhibition of secondary metabolites of *A. triplinervis* in receptors of the enzyme acetylcholinesterase and receptors of the juvenile hormone was evaluated. Acetylcholinesterase is an essential enzyme in the insect's nervous system responsible for the hydrolysis of the neurotransmitter acetylcholine, and the juvenile hormone plays a crucial role in the development and reproduction of insects. AChE is the main compound in which nerve impulses are transmitted between cells through cholinergic synapses and its inhibition by essential oils causes super stimulation of neurons, muscle spasms, convulsion, paralysis, and death in the insects (López and Pascual-Villalobos, 2010). Secondary metabolites can influence the hormonal regulation of *A. aegypti* and cause sublethal effects at the physiological, morphological, and behavioural levels that compromise the insect's development cycle, such as interruption of reproduction and a decrease in longevity (Alomar et al., 2021).

In our previous studies, we reported the larvicidal activity of nanoformulations containing the essential oil of *A. triplinervis* morphotypes in *A. aegypti*, which showed low toxicity in non-target mammals (Rodrigues et al., 2021). In this study, we hypothesized that *A. triplinervis* essential oil nano-emulsion can be used to control *A. aegypti* in the adult stage. This study aims to evaluate the potential adulticide in *A. aegypti* through molecular docking of essential oils and biological tests of the nano-emulsions from *A. triplinervis* morphotypes, and acute dermal toxicity in Swiss albino mice (*Mus musculus)* of the nanoformulations.

2. Materials and methods

2.1. Molecular docking simulations of essential oils from *A. triplinervis* morphotypes

2.1.1. Selection of enzymes and inhibiting structures

The crystallographic structure of *Drosophila Melanogaster* acetylcholinesterase (AChE) complexed with 9- (3-iodobenzylamino) −1,2,3,4-tetrahydroacridine (I40) and *Aedes aegypti* juvenile hormone complexed with methyl (2E, 6E) − 9 – [(2R) −3,3-dimethyloxiran-2-yl] −3,7-dimethylnona-2,6-die noate (JH3) were downloaded from the Protein Data Bank (PDB) with the respective codes PDB 1QON (resolution 2.7 Å) and PDB 5 V13 (1.87 Å resolution). I40, JHIII, and pyriproxyfen were used as positive control ligands in molecular docking studies based on the standard protocol established by Ramos and co-workers (Ramos et al., 2020).

There is no crystallographic structure of *A. aegypti* AChE deposited in the Protein Data Bank. In this study, *D. melanogaster* AChE was used, which has a 39% similarity with *A. aegypti* AChE (Ramos et al., 2020).

Table 1 Data from protocols used for molecular docking validation.

Enzyme	Inhibitor	Coordinates of the Grid Center	Grid Size (Points)
AChE (PDB code: 1QON)	9-(3-Iodobenzylamino)-1,2,3,4-Tetrahydroacridine	X = 34.279 Y = 67.55 Z = 9.28	42 x 26 y 16 z
Juvenile hormone (PDB code: 5 V13)	methyl (2E,6E)-9-[(2R)-3,3-dimethyloxiran-2-yl]-3,7-dimethylnona-2,6-dienoate	X = 213.483 Y = 2.850 Z = 353.222	42 x 40 y 24 z

2.1.2. Docking study with AutoDock 4.2/Vina 1.1.2 via graphical interface PyRx (Version 0.8.30)

The ligands and protein structures were prepared using the Discovery Studio 5.0 software. In the docking study of AChE (*D. melanogaster*) and Juvenile Hormone, the complexed ligands were used in the AutoDock 4.2/Vina 1.1.2 software, and then in PyRx 0.8.30 (https://pyrx.sourceforge.io). The validation of the molecular docking of the ligand was performed by comparison between the crystallographic ligand and the best conformation obtained with molecular docking (structure of the PDB ID: 1QON), based on the RMSD value. The ×, y, and z coordinates of the receivers are determined according to the average region of the active site, and the coordinates used for the center of the grid can be seen in Table 1.

2.2. Evaluation of adulticidal activity of A. triplinervis nano-emulsions against A. aegypti

The susceptibility of *A. aegypti* adults was assessed using the Centers for Disease Control and Prevention (CDC) bottle bioassay (Brogdon and Chan, 2013) to determine the dose of insecticide that kills 100% of susceptible mosquitoes (diagnostic dose) within a specific time (diagnostic time).

Nano-emulsions were diluted in acetones in concentrations of 150, 100, and 50 $\mu g.mL^{-1}$, and 1 mL of each solution was applied inside Wheaton bottles (250 mL). Nano-emulsion produced only with the blend of surfactants was used as a negative control and malathion at 50 $\mu g.mL^{-1}$ was used as a positive control. Solutions were distributed in all internal areas of the bottles through rotation movements in different directions. The bottles were opened at room temperature to evaporate the acetone.

Twenty-five adult females of *A. aegypti* were gently inserted into each Wheaton with an aspirator, and mortality was assessed every 15 min for a period of 180 min. Mosquitoes that did not stand or slide along the curvature of the bottle were considered dead.

The bioassay was performed in quadruplicate and the data was validated according to the mortality percentage of the negative control. When the mortality of the negative control was greater than 10% the tests were discarded. In the case of the tests in which the mortality of the control was between 3% and 10%, the mortality was corrected by Abbott's formula (Consoli and Oliveira, 1994).

$$Corrected\ mortality = \frac{(mortality\ in\ test\ bottles\ [\%] - mortality\ in\ control\ bottle\ [\%]) \times 100}{(100\% - mortality\ in\ control\ bottle\ [\%]}$$

2.3. Evaluation of acute toxicity of A. triplinervis essential oils Nano-emulsions

This study was approved by the Research Ethics Committee of Universidade Federal do Amapá (CEP – Unifap – 004/2019). All procedures were performed by international animal care protocols and national animal testing regulations. The experiments used male and female, 12-week-old Swiss albino mice (*Mus musculus*), provided by the Multidisciplinary Center for Biological Research in the Area of Science in Laboratory Animals (CEMIB).

The animals were kept in polyethylene cages at a controlled temperature (22 °C) over a 12 h of light or dark cycle and had free access to food and water, on experiment day when they had private access to food 3 h before, with restitution 1 h after nano-emulsion or negative control treatment.

Acute oral toxicity of the nano-emulsions was performed with 3 experimental groups (morphotype A essential oil nano-emulsion (MAEON), morphotype B essential oil nano-emulsion (MBEON), and negative control), each group with 6 animals (3 males and 3 females).

The test was performed according to Guideline 402 of the Organization for Economic Co-operation and Development (OECD, 2017) for acute toxic dose class testing. On the day before administration of the nano-emulsion, all the fur was removed from the dorsal (at least 10% of the total body surface area). Nanoformulations or negative control were diluted in water at 2,000 $mg.kg^{-1}$ (limit of 1 mL of the solution) and applied uniformly over the exposed area of the dorsal.

Swiss albino mice (*Mus musculus*) were observed at 30, 60, 120, 240, and 360 min after application of the nano-emulsion and daily for 14 days. Behavioural changes were assessed and recorded: in skin and fur, eyes and mucous membranes, general activity, vocal frenzy, irritability, touch response, response to tail stimulus, contortion, posterior train position, straightening reflex, body tone, grip strength, ataxia, auricular reflex, corneal reflex, tremors, convulsions, anaesthesia, lacrimation, ptosis, urination, defecation, piloerection, hypothermia, breathing, cyanosis, hyperaemia, and death. Water consumption (mL) and food intake (g) were evaluated daily, and body weight every 3 days.

Animals were sacrificed on the fourteenth day in a CO_2 chamber, obeying the ethical principles of animal experimentation. Skin, liver, lung, and kidney were removed for macroscopic and histopathological analysis.

2.4. Histopathological analysis

Organs were fixed in a 10% formalin buffer solution, routinely processed, and embedded in paraffin. Paraffin sections (5 μm) were stained with haematoxylin and eosin. The slides were examined under a light microscope and the magnified images of the tissue structure were captured for further study (Calleja et al., 2013).

2.5. In silico pharmacokinetic and toxicological properties of essential oils from A. triplinervis morphotypes

The molecules of *A. triplinervis* essential oils were submitted to the QikProp software to obtain pharmacokinetic properties. The parameters generated by the software allowed us to select the candidate having a parameter of 95% of approximation with pharmacokinetic characteristics of drugs already described in the literature, giving reliability to the generated data. The toxicity profile of the molecules was performed using DEREK software. DEREK is *in silico* toxicological prediction software used for drug design purposes (Ramos et al., 2020).

2.6. Toxicity risk assessment

ProTox, a virtual lab for the prediction of toxicities of small molecules as well as a useful tool to identify any undesirable toxic properties of our molecules, was used (Costa et al., 2019) (see https://tox.charite.de/protox_II/). The prediction was based on functional group similarity for the query molecules with the *in vitro* and *in vivo* contained in the database. Toxic properties such as LD_{50} values in mg/kg and toxicity class were determined.

2.7. Prediction of metabolites in metatox

In MetaTox application, the prediction of substrate modification is based on the rules of transformation. The predictions of metabolite formation were integrated into the MetaTox web service to evaluate the generation and modification of xenobiotic metabolism pathways (https://www.way2drug.com/mg). The LD_{50} values of acute rat toxicity are calculated for a parent compound and each of the generated metabolites, considering Pa > Pi as an exclusion criterion (Rudik et al., 2017).

2.8. Statistical analysis

The data were organized into mean and standard deviations and analysed using a one-way Analysis of Variance followed by Bonferroni's multiple comparison test in GraphPad Prism Software v.7 (San Diego, California, USA) with a 95% confidence limit.

3. Results

The docking validation was done through the conformational similarity between the inhibitors used as positive control I40 and JHIII complexed with AChE or juvenile hormone and their crystallographic information. The root-mean-squared distance (RMSD) values were 0.79 Å for I40 and 1.72 Å for JHIII and indicate that the docking protocol is optimized and satisfactory, as the RMSD was lower than 2 Å (Santos et al., 2018). The best results can be seen in Fig. 1.

Interactions between I40 and AChE observed *in silico* reproduced the interactions described *in vitro*, as π-π planar interaction with Trp 83 on β-sheet, π-π with the Tyr 370 on α-helix, π-π interaction with Tyr 71 on α-helix, hydrogen bond with Hys 480, and hydrophobic interactions with Tyr 370, among others (Harel et al., 2000).

The interactions between JHIII and juvenile hormone observed *in silico* reproduced the hydrophobic interactions described *in vitro* and validate the theoretical model of molecular docking, such as Tyr 33, Leu 37, Val 51, Trp 53, Tyr 64, Val 65, Val 68, and Tyr 129 in the α-helix; Leu 74 and Phe 144 on the β-sheet (Kim et al., 2017).

The binding affinities of terpenes found in the essential oils of each morphotype of *A. triplinervis* (Table 2) complexed with acetylcholinesterase and juvenile hormone receptors were predicted and compared with the binding affinity of inhibitors I40, JHIII, and pyriproxyfen to select secondary metabolites with an affinity for binding equal to or greater than positive controls. Five compounds showed potential inhibition of acetylcholinesterase receptors: aciphyllene, α-muurulene, and γ-gurjunene from morphotype A essential oil, and valencene and α-cedrene epoxide from morphotype B essential oil, as shown in Fig. 2.

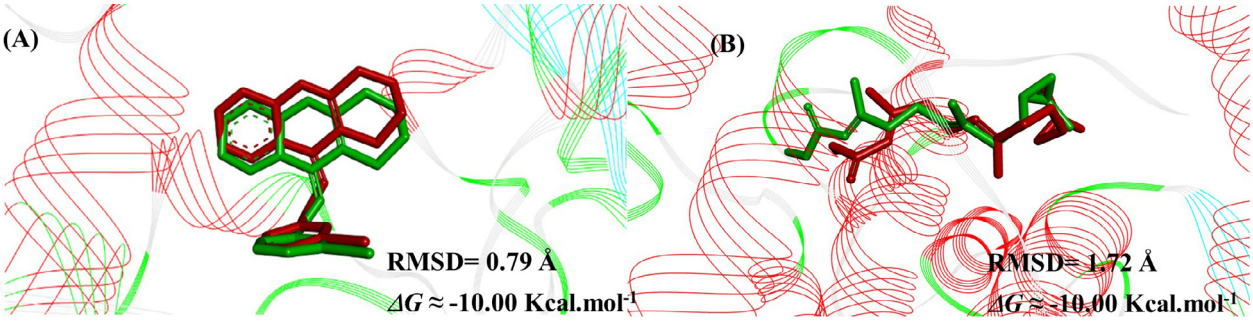

Fig. 1 Superpositions of the crystallographic poses (in green) with the docked ones (in red) of the compounds (A) I40 and (C) JHIII, and respective RMSD and ΔG values.

Table 2 Chemical composition of essential oil of morphotype A (MAEO) and morphotype B (MBEON) of Ayapana triplinervis.

Chemical Structure	Name	MAEO (%)	MBEO (%)	Reference
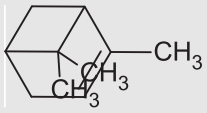	α-Pinene	0.93	1.25	Rodrigues et al. (2021)
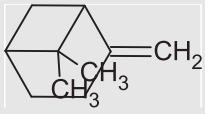	β-Pinene	2.16	2.26	
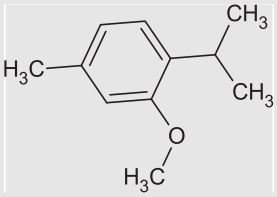	Thymol Methyl Ether	0.68	–	
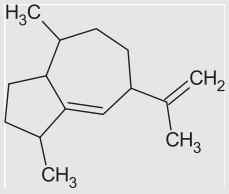	α-Gurjunene	0.98	0.41	
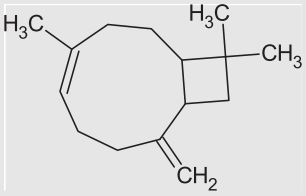	β-Caryophyllene	45.93	–	
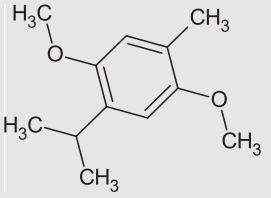	Thymohydroquinone Dimethyl Ether	32.93	84.53	
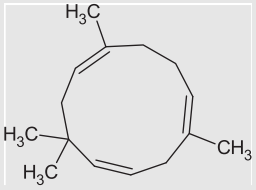	α-Humulene	1.60	1.11	
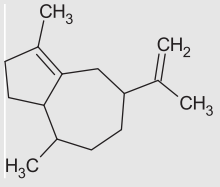	Aciphyllene	0.53	–	
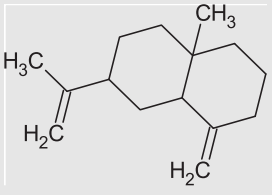	β-Selinene	0.88	0.41	

(*continued on next page*)

Table 2 (*continued*)

Chemical Structure	Name	MAEO (%)	MBEO (%)	Reference
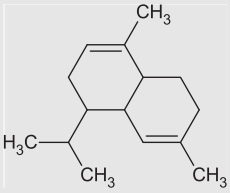	α-Muurulene	0.45	–	
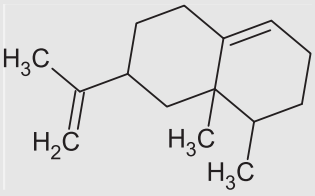	Valencene	–	0.53	
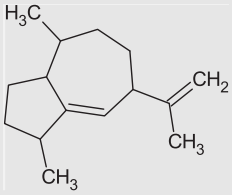	γ-Gurjenene	0.64	–	
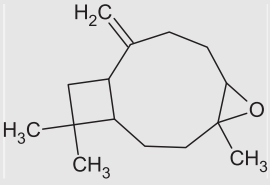	Caryophyllene Oxide	0.76	0.67	
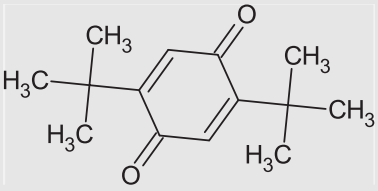	2,5-Di-Tert-Buthyl-1,4-Benzenoquinone	4.22	1.82	
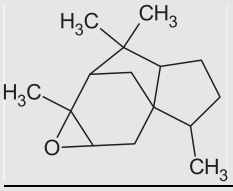	α-Cedrene Epoxide	–	0.93	

Aciphyllene was the most promising metabolite that showed a binding affinity with the acetylcholine complex of -9.3 Kcal.mol^{-1}, proceeded by γ-gurjunene, and valencene, which together have strong interaction in docking with the amino acid residues Tyr 71, Trp 83 and Tyr 370 that represent the acetylcholinesterase catalytic site and were similar to the *in vitro* experimental results described in the literature (Costa et al., 2019). These interactions reproduced the molecular ones observed in the positive controls and indicate inhibition of acetylcholinesterase receptors, as shown in Fig. 3:

Four compounds showed a potential binding affinity for the inhibition of *A. aegypti* juvenile hormone receptors, among them α-muurulene, α-cedrene epoxide, and γ-gurjunene found only in morphotype A, and β-selinene in morphotype A and morphotype B, as shown in Fig. 4:

Hydrophobic interactions described in the scientific literature for *in vitro* study were similar to those observed in docking for α-muurulene, β-selinene, and α-cedrene epoxide including those of Tyr-64, Trp-53, Val-65, Val-68, and Tyr-33 (Kim et al., 2017) and indicate the inhibition of *A. aegypti* juvenile hormone receptors, as shown in Fig. 5:

The major compounds Thymohydroquinone Dimethyl Ether and β-caryophyllene did not predict significant binding affinity to inhibit acetylcholine and juvenile hormone receptors when compared to positive controls. However, molecular docking predicted that minor compounds present in morphotype A essential oil (α-muurulene, α-cedrene epoxide γ-gurjunene, and β-selinene) have greater potential to bind to acetylcholinesterase enzyme and juvenile hormone receptors when compared to morphotype B essential oil (β-selinene)

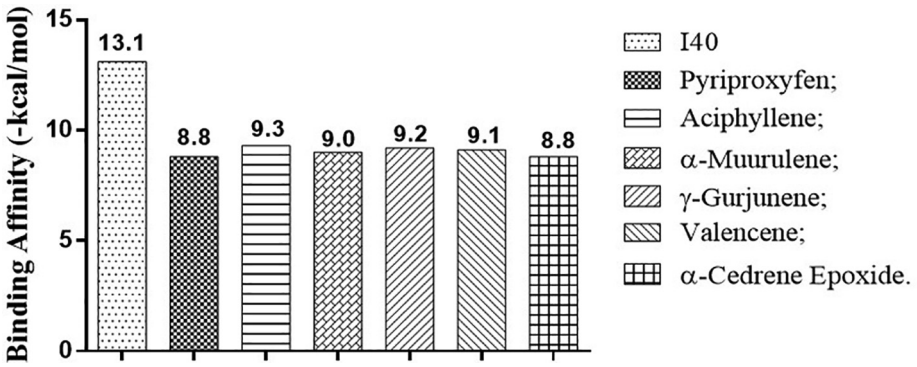

Fig. 2 Results of binding affinity of the compounds os *A. triplinervis* morphotypes with the acetylcholinesterase (*Drosophila Melanogaster*) receptor (PDB ID 1QON).

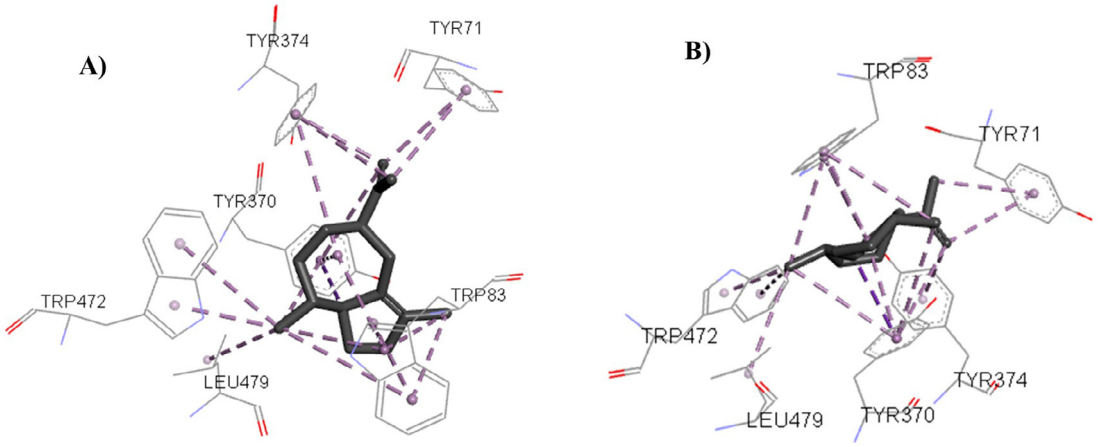

Fig. 3 Interactions between the *Drosophila Melanogaster* acetylcholinesterase active site and the compounds (A) Aciphyllene and (B) γ-Gurjunene.

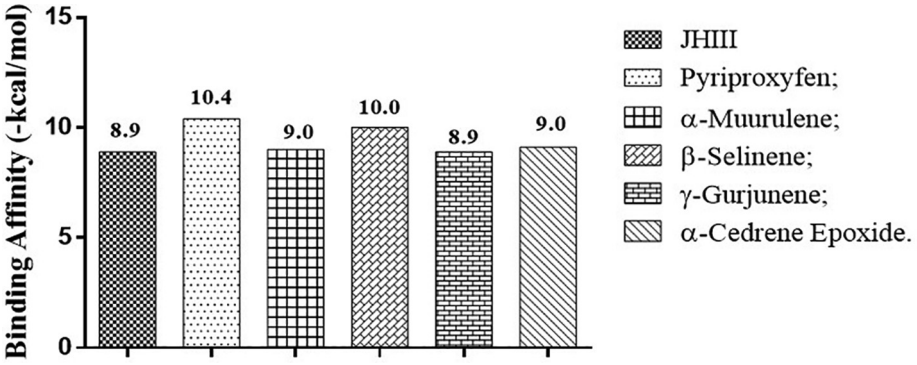

Fig. 4 Results of binding affinity of the compounds with the *A. aegypti* juvenile hormone receptor (PDB ID 5V13).

through the individual or synergistic action of secondary metabolites.

The Centers for Disease Control and Prevention (CDC) bottle bioassay was used to assess whether nano-emulsions can help control the *A. aegypti* vector. The bioassay assesses the time and dose at which nano-emulsions arrive at the target site and cause mortality (Aïzoun et al., 2014).

The nano-emulsions used here were prepared according to our previous studies and demonstrated kinetic stability and monomodal distribution. Morphotype A essential oil nano-emulsion (MAEON) had a particle diameter equal to 101.400 ± 0.971 nm (PdI = 0.124 ± 0.009 and ZP = -19.300 ± 0.787 mV). Morphotype B essential oil nano-emulsion (MBEON) showed particle size 104.567 ± 0.416 nm (PdI = 0.168 ± 0,016 and ZP = -27.700 ± 1.307 mV).

The results showed that 100% of *A. aegypti* was susceptible to MAEON at 150 $\mu g.mL^{-1}$ within 15 min of exposure. At the

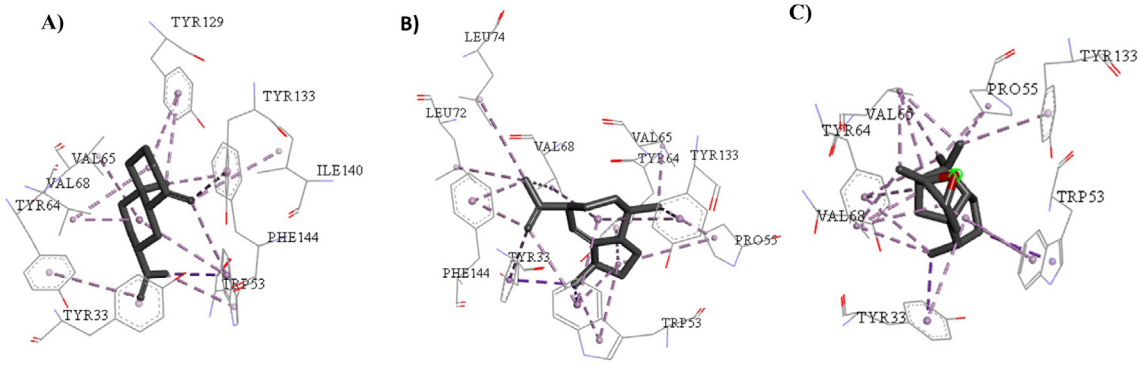

Fig. 5 Interactions between the active site of *A. aegypti* juvenile hormone with (A) α-muurulene, (B) β-selinene and (C) α-cedrene epoxide.

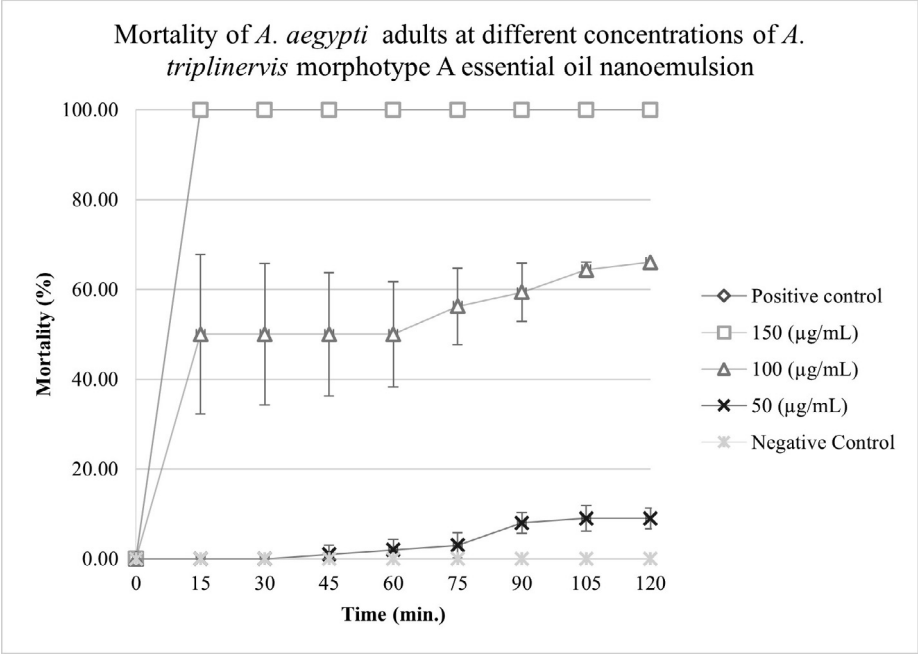

Fig. 6 Mortality of *A. aegypti* adults as a function of time in different concentrations do *A. triplinervis* morphotype A essential oil nanoemulsion (MAEON). Malathion at 50 $\mu g.mL^{-1}$ was used as a positive control.

lowest concentration evaluated, 50 $\mu g.mL^{-1}$, there was no mortality at the same time of exposure. There was no statistically significant difference between the concentration of MAEON at 150 $\mu g.mL^{-1}$ and the positive control (p-value < 0.05, F = 32.602). MAEON showed a diagnostic dose of 150 $\mu g.mL^{-1}$ in the diagnostic time of 15 min, as shown in Fig. 6.

For MBEON, the results indicate that 100% of *A. aegypti* were susceptible to 150 $\mu g.mL^{-1}$ in 45 min of exposure. In the same exposure period, the lowest concentration (50 $\mu g.mL^{-1}$) showed a mortality of approximately 0%. There was no statistically significant difference between the concentration of MBEON at 150 $\mu g.mL^{-1}$ and the positive control (p-value < 0.05, F = 32.172). MBEON presented a diagnostic dose of 150 $\mu g.mL^{-1}$ in a diagnostic time of 45 min, as shown in Fig. 7.

MAEON and MBEON acted effectively in the control of *A. aegypti* at the same diagnostic dose, but at different diagnostic times and, according to the World Health Organization (World Health Organization, 2016), it is possible to conclude that *A. aegypti* adults were susceptible to *A. triplinervis* nano-emulsion.

The mosquito has a genetic preference to enter homes, blood feed on humans, and reproduce in relatively clean water in urban environments (Crawford et al., 2017). Due to the anthropophilic behaviour of *A. aegypti*, the acute dermal toxicity of *A. triplinervis* nano-emulsions was evaluated in non-target mammals.

During the assessment of acute toxicity, no mortality was observed in Swiss albino mice (*Mus musculus*) treated with MAEON and MBEON. Hippocratic screening indicated that animals treated with MAEON show symptoms of irritability, whereas animals treated with MBEON showed signs of irritability, itching, and corneal reflex, as shown in Table 3.

The physiological parameters did not indicate significant differences in water consumption and food intake in the

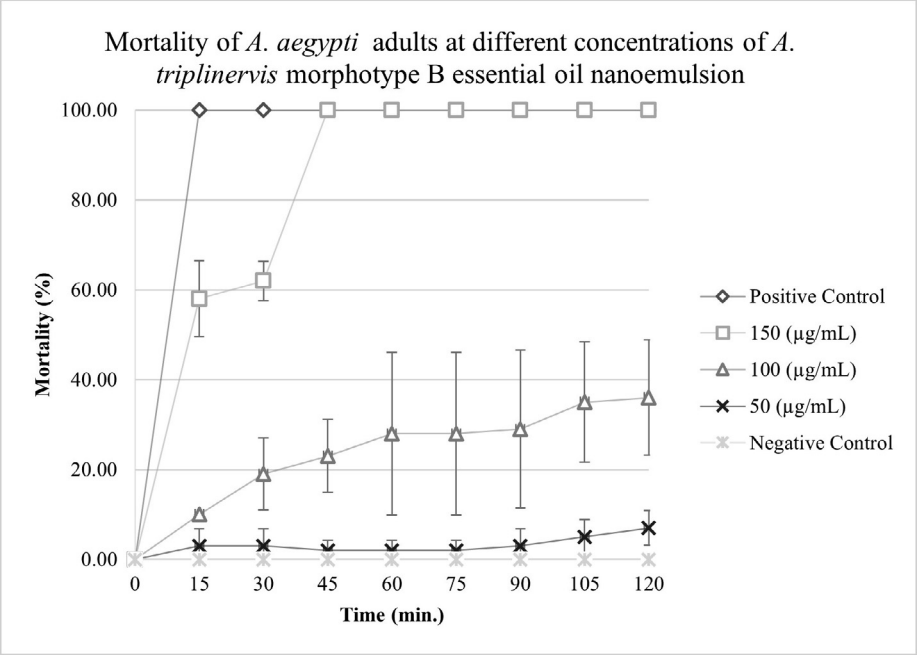

Fig. 7 Mortality of *A. aegypti* adults as a function of time in different concentrations do *A. triplinervis* morphotype B essential oil nanoemulsion (MBEON). Malathion at 50 $\mu g.mL^{-1}$ was used as a positive control.

Table 3 Effect of oral administration of MAEON and MBEON (2000 $mg.kg^{-1}$) on behavioral parameters of Swiss albino mice (*Mus musculus*) during acute dermal toxicity assessment.

Groups	Gender	Number of animals	Number of Death	Symptoms
Control	Males	3	0	–
	Female	3	0	–
MAEON	Males	3	0	Irritability
	Female	3	0	Irritability
MBEON	Male	3	0	Irritability, itching
	Female	3	0	Corneal reflex

Table 4 Physiological parameters of Swiss albino mice (*Mus musculus*) treated with MAEON and MBEON at 2000 $mg.kg^{-1}$. Values are expressed as mean ± standard deviation (n = 3). Statistical significance was calculated using One-way Anova followed by Bonferroni's multiple comparison test ($p < 0.01$).

Parameter	Control		MAEON		MBEON	
	Male	Female	Male	Female	Male	Female
Water (mL)	13.71 ± 4.61	11.47 ± 3.19	12.80 ± 4.96	11.86 ± 4.83	11.04 ± 4.19	12.30 ± 4.12
Food (g)	6.67 ± 1.17	5.76 ± 0.66	6.80 ± 0.88	7.81 ± 1.96	6.20 ± 0.77	6.94 ± 1.18
Weight (g)	31.81 ± 1.82	24.25 ± 2.10	30.30 ± 2.69	25.84 ± 1.69	29.72 ± 2.97	25.85 ± 1.44

MAEON and MBEON groups compared to the control group. The animals showed weight gain in the MAEON and MBEON groups and differed from the control group, as shown in Table 4:

The evaluation of the relative weight of the organs showed that the livers of the group treated with MAEON increased significantly (*$p < 0.05$) when compared to the control group. Kidneys, Hearts, and lungs did not show changes in relative weight. The relative weights of the livers, kidneys, Hearts, and lungs of male and female mice treated with MAEON and MBEON are shown in Table 5.

In the histopathological evaluation of the dermis, acantholysis, infiltrated neutrophils, thickening of the corneal layer, formation of crusts, and presence of inflammatory cells were not found after the fourteenth day of treatment. Lungs, kid-

Table 5 Effect of MAEON and MBEON at 2000 $mg.kg^{-1}$ on the weight of different Swiss albino (*Mus musculus*) organs after 14 days of treatment. Values are expressed as mean ± standard deviation (n = 3). Statistical significance was calculated using One-way Anova followed by Bonferroni's multiple comparison test ($p < 0.05$).

Organs (%)	Control		MAEON		MBEON	
	Male	Female	Male	Female	Male	Female
Liver	5.99 ± 0.59	6.76 ± 0.81	7.52 ± 0.72	6.93 ± 0.86	7.54 ± 0.16*	6.73 ± 0.37
Kidneys	0.91 ± 0.05	0.93 ± 0.15	0.98 ± 0.04	0.93 ± 0.21	0.95 ± 0.05	0.80 ± 0.06
Heart	0.48 ± 0.01	0.72 ± 0.11	0.51 ± 0.31	0.55 ± 0.06	0.56 ± 0.02	0.64 ± 0.10
Lungs	0.65 ± 0.15	0.82 ± 0.18	0.87 ± 0.24	0.80 ± 0.16	0.65 ± 0.08	0.81 ± 0.24

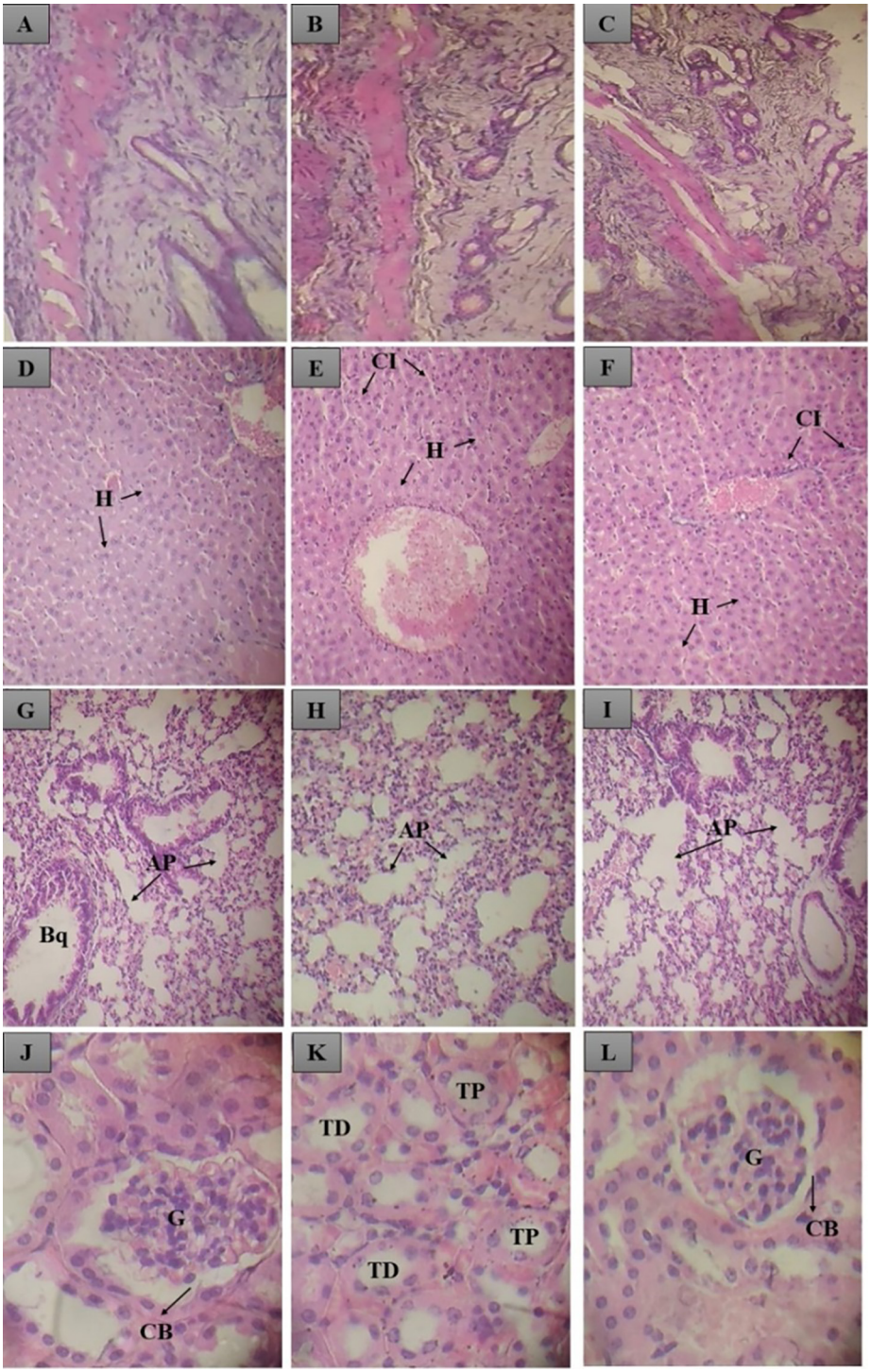

Fig. 8 Histological section of *Mus musculus* treated cutaneously with the control (Tween 80 + 20), MAEON and MBEON. In A, B and C there is a normal region of the dermis of the animal treated with the control, MAEON and MBEON, respectively. In D, the normal liver of an animal treated with the control; in E and F, the liver of an animal treated with MAEON and MBEON, where normal hepatocytes (H) and the presence of inflammatory cells (CI) are observed**.** Em G, H e I, the lung of a normal animal treated with the control, MAEON and MBEON, where pulmonary alveoli (AP) and bronchioles (Bq) are observed. In J, K and L, normal kidney of an animal treated with the control, MAEON and MBEON, where the glomerulus (G), the Bowmam capsule (CB), distal tubule (TD), proximal tubule (TB) are observed.

neys, livers, and dermis showed normal appearances. However, the presence of inflammatory cells was identified in the liver of animals treated with MAEON and MBEON. No histopathological changes were observed in the control group, as shown in Fig. 8:

A virtual prediction was performed using the ProTox server to investigate which compounds present in essential oils could be associated with the reported inflammation in the mouse liver. ProTox uses the two-dimensional similarity method to relate the chemical structure to the results available in the scientific literature database to predict the interactions of toxicophoric groups, determine the LD_{50} in rodents, and suggest a mechanism for the development of toxicity (Drwal et al., 2014). The analysis did not predict the hepatotoxicity associated with essential oil constituents of *A. triplinervis* morphotypes, as can be seen in the following Table 6:

Another *in silico* toxicity prediction was made using the Deductive Estimation of Risk from Existing Knowledge (DEREK) 10.0.2 program (Ridings et al., 1996). We have considered DEREK alerts of toxicity involving the human species and also classified them as plausible in mammals. DEREK program qualitatively predicts the toxicity of the compounds through a specialist system that focuses attention on the toxic action of chemical compounds.

In addition to toxicity, DEREK software can be used to identify aspects related to skin sensitization, irritation, and neurotoxicity (Ramos et al., 2020). Table 7 shows the results of toxicity predictions by the identification of toxicophore groups of *A. triplinervis* essential oils.

Skin irritation and sensitization were the toxicological parameters found in DEREK analyses. Therefore, these compounds were selected to evaluate the prediction of the biotransformation metabolism of xenobiotics in the liver that can cause toxicity through the MetaTox web server. Metabolism can increase the toxicity of a compound, in which case it is referred to as an activation reaction. More frequently, metabolism decreases the toxicity of a compound through a detoxification reaction.

A new freely available web-application MetaTox (https://www.way2drug.com/mg) for the prediction of xenobiotic metabolism and calculation of metabolites toxicity based on the structural formula of chemicals has been developed. The calculation of probability for generated metabolites is based on the analyses of "structure-biotransformation reactions" and "structure-modified atoms" relationships, using a Bayesian approach. Prediction of LD_{50} values is performed by GUSAR software for the parent compound and each of the generated metabolites using QSAR models created for acute rat toxicity with the intravenous type of administration (Rudik et al., 2016).

The results showed 20 xenobiotics metabolites from caryophyllene oxide, 19 from α-cedrene epoxide, and 4 from

Table 6 *In silico* prediction of hepatotoxicity of the chemical components of *A. triplinervis* using the ProTox server.

Compounds	LD_{50} Toxic[a]	Toxicity class[b]	Target	Prediction	Probability
α-pinene	3700	V	Hepatotoxicy	Inactive	0.86
β-pinene	4700	V	Hepatotoxicy	Inactive	0.80
Thymol methyl ether	880	IV	Hepatotoxicy	Inactive	0.74
γ-gurjunene	5000	V	Hepatotoxicy	Inactive	0.78
β-caryophyllene	500	V	Hepatotoxicy	Inactive	0.80
Thymohydroquinone dimethyl ether	880	IV	Hepatotoxicy	Inactive	0.72
α-humulene	4400	V	Hepatotoxicy	Inactive	0.83
Aciphyllene	4690	V	Hepatotoxicy	Inactive	0.73
β-selinene	5000	V	Hepatotoxicy	Inactive	0.79
α-muurulene	4400	V	Hepatotoxicy	Inactive	0.83
Valencene	5000	V	Hepatotoxicy	Inactive	0.76
γ-gurjunene	5000	V	Hepatotoxicy	Inactive	0.73
Caryophyllene oxide	5000	V	Hepatotoxicy	Inactive	0.80
2,5-di-*tert*-butyl-1,4-benzenoquinone	2400	V	Hepatotoxicy	Inactive	0.65
α-cedrene epoxide	5000	V	Hepatotoxicy	Inactive	0.83

[a] Values in mg/kg body weight.

[b] Class I: fatal if swallowed ($LD_{50} \leq 5$); Class II: fatal if swallowed ($5 < LD_{50} \leq 50$); Class III: toxic if swallowed ($50 < LD_{50} \leq 300$); Class IV: harmful if swallowed ($300 < LD_{50} \leq 2000$); Class V: may be harmful if swallowed ($2000 < LD_{50} \leq 5000$); Class VI: non-toxic ($LD_{50} > 5000$).

Table 7 Toxicity prediction by the identification of toxicophores groups and LD_{50} for *A. triplinervis* essential oils.

Compounds	Toxicity Prediction Alert (Lhasa Prediction)	Toxicophoric Group	Toxicity alert
Caryophyllene oxide	Irritation (of the eye) in human, mouse and rat Irritation (of the skin) in human, mouse and rat Skin sensitisation in human, mouse and rat	Epoxide	PLAUSIBLE
2,5-Di-*tert*-buthyl-1,4-benzoquinone	Skin sensitisation in human, mouse and rat	Quinone	PLAUSIBLE
α-cedrene epoxide	Irritation (of the eye) in human, mouse and rat	Epoxide	PLAUSIBLE

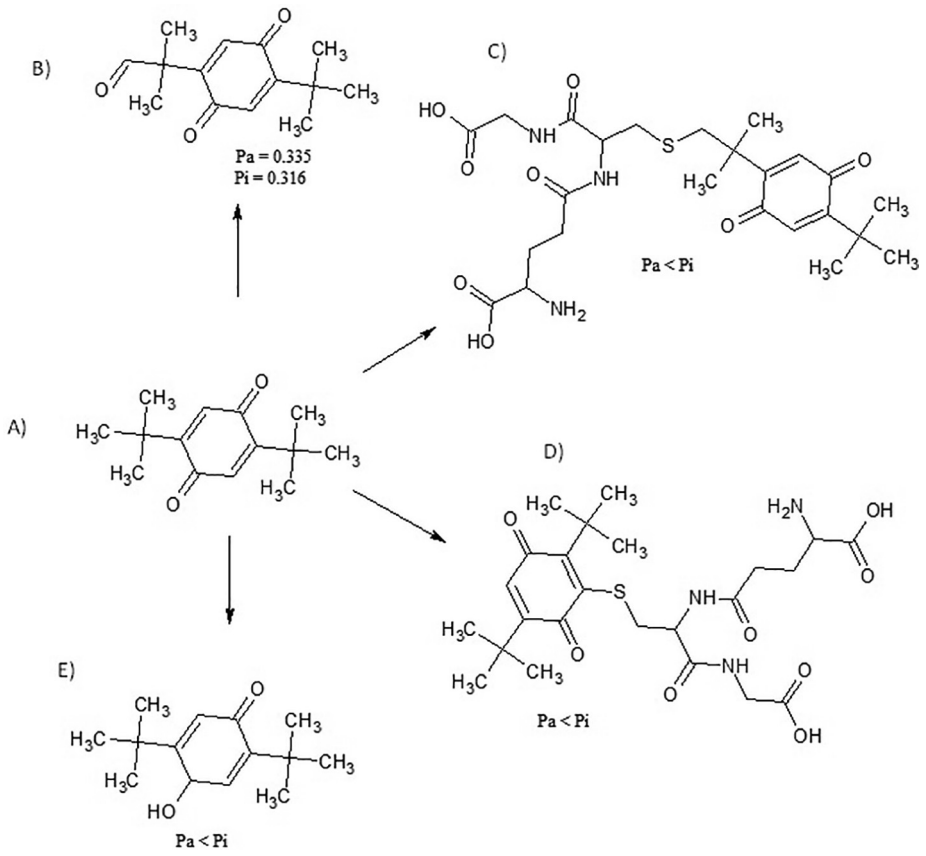

Fig. 9 Biotransformation of (A) 2,5-di-*tert*-buthyl-1,4-benzenoquinone through (B) C-oxidation, (C) Glutathionation, (D) Glutathionation, and (E) Hydrogenation. Pa and Pi represent the probability of xenobiotic metabolites being active (Pa) or inactive (Pi) for hepatotoxicity.

2,5-di-*tert*-buthyl-1,4-benzenoquinone. The only xenobiotics metabolite that showed a probability of promoting a hepatotoxic effect was that derived from biotransformation 2,5-di-*tert*-buthyl-1,4-benzenoquinone through C-oxidation by cytochrome oxidase enzymes (Croom, 2012) and presented LD_{50} = 868.49 $mg.kg^{-1}$, as shown in Fig. 9.

4. Discussion

This study predicted that acyphyllene, α-muurulene, γ-gurjunene, valencene, and α-cedrene epoxide terpenes have the potential to inhibit *D. Melanogaster* acetylcholinesterase receptors through the catalytic site. These data are in accordance with studies available in the literature that demonstrate the inhibitory action of terpenes on the acetylcholine enzyme through docking molecular (Khanikor, 2013; Silva et al., 2014).

The molecular docking carried predicted the action of the essential oils of *A. triplinervis* morphotypes on *D. melanogaster* acetylcholinesterase receptors through complexation with the enzyme's catalytic site. As the literature reports that different enzymes belonging to the cholinesterase family share the same catalytic mechanism (Moralev et al., 2001), it is possible to infer that the essential oils of *A. triplinervis* morphotypes can also inhibit the acetylcholinesterase enzyme of *A. aegypti*.

The insecticidal activity of several essential oils has demonstrated a correlation with inhibition of the enzyme acetylcholinesterase (Seo et al., 2015). *Perilla frutescens* essential oil showed insecticidal activity against *Drosophila suzukii* (Park et al., 2016), *Citrus sinensis* essential oil showed insecticidal activity against *Tribolium confusum, Callosobruchus maculatus, and Sitophilus oryzae* (Oboh et al., 2017), and *Ocimum tenuiflorum* essential oil showed insecticidal activity against *Sitophilus orzyae* (Bhavya et al., 2018). All of these examples showed high inhibition of the AChE enzyme.

Another important strategy for controlling *A. aegypti* is focused on the morphogenesis and reproduction of insects by the regulation of juvenile hormones for the development of new insecticides (Cusson et al., 2013; Moralev et al., 2001). Our results showed that α-muurulene, β-selinene, γ-gurjunene, and α-cedrene epoxide have the potential to act as regulators of the juvenile hormone. The prediction *in silico* of this study is in agreement with experimental tests that demonstrated that terpenes from essential oils can block egg maturation in female mosquitos and disrupt the expression of the Juvenile Hormone-induced gene (Chokechaijaroenporn et al., 1994; Lee et al., 2018).

This study reported for the first time in the literature the evaluation of the adulticidal activity of nano-emulsion in *A. aegypti* using CDC bottle bioassay and reported exclusively the nanoinsecticidal potential of formulations based on *A. triplinervis*. Thus, it is possible to conclude that the essential oils of *A. triplinervis* morphotypes can be used in the chemical control of *A. aegypti* adults through the inhibitory properties

of acetylcholinesterase enzyme and juvenile hormone receptors.

Studies regarding the adulticidal activity in *A. aegypti* have shown that *Lippia origanoides* essential oil (Carvacrol 50.6%) killed 100% at 300 $\mu g.mL^{-1}$ in 60 min of exposure (Castillo et al., 2017; Chokechaijaroenporn et al., 1994). In another study with *Melaleuca quinquenervia* essential oil (28.7% 1,8-cienole and 25.2% viridiflorol) killed 100% of *A. aegypti* at 40,000 $\mu g.mL^{-1}$ in 30 min.

From the point of view of nanoformulations, nanoparticles based on *Heliotropium indicum* presented mortality of 98.2% of *A. aegypti* at 250 $\mu g.mL^{-1}$ in 24 h of exposure (Castillo et al., 2017; Veerakumar et al., 2014). In another study, nanoparticles based on *Olea europaea* showed mortality of 73.3% in *D. melanogaster* at 200 $\mu g.mL^{-1}$ in 168 h of exposure (Araj et al., 2015; Veerakumar et al., 2014).

Comparing these results above with the dose and diagnostic time found for MAEON and MBEON, the nanoformulations based on *A. triplinervis* morphotypes essential oils can be used in the chemical control of *A. aegypti* and, as shown in the molecular docking simulations, with possible insecticidal action through inhibition of the catalytic site in enzyme acetylcholinesterase receptors and juvenile hormone receptors.

Aggregates of small lipophilic molecules or colloidal structures can influence the structure-ligand binding, producing non-specific mechanisms of action or the induction of conformational changes that affect the protein and can represent false-positive results. Thus, it is suggested the future perspectives for this study to evaluate the influence of the critical concentration of nano-emulsion colloidal aggregates on AChE and juvenile hormone receptors through molecular dynamics techniques (Ghattas et al., 2020; Vázquez et al., 2020).

Plant secondary metabolites have advantages as biopesticides because they are easily available, inexpensive, biodegradable, don't leave chemical residues, and offer greater security to non-target species (Gupta et al., 2019). When secondary metabolites with insecticidal action are stabilized within a nanotechnological system, nanoinsecticides are more efficient due to the greater surface area, solubility, mobility, and low toxicity without the presence of organic solvents than the conventional use of many commercial pesticides. (Durán et al., 2016).

Nanoinsecticides can come into contact with non-target mammals through inhalation, the digestive tract, or skin absorption. The permeability of MAEON and MBEON over the skin can occur through pinocytosis by the transcellular mechanism and provoke its deleterious effects (Rai et al., 2018).

Corneal reflex was one of the toxicological effects found in the hippocratic screening and indicates an action on the central nervous system of nano-emulsions. This result is in line with what is reported in the literature, which describes the sedative, anxiolytic and antidepressant effects of *A. triplinervis* extracts (Melo et al., 2013).

Nano-emulsions caused subtle toxicological effects on the liver of mice that could be seen through the presence of inflammatory cells. Different results of this study showed a hepatoprotective effect of methanolic extract of the species (Bose et al., 2007).

The initial *in silico* prediction did not indicate a hepatotoxic effect of the chemical constituents of essential oils, indicating action resulting from the synergistic effect of essential oil compounds or the action of their biotransformation in the liver. However, the analysis of xenobiotic metabolism showed hepatotoxic action of the biotransformation of 2,5-di-*tert*-butyl-1,4-benzenoquinone. This biotransformation may have occurred through the action of the cytochrome P450 enzyme and is extremely selective in the oxidation of substrates as the first defense mechanism (Kliewer et al., 2002). However, it was not possible to state that nano-emulsions containing essential oil from *A. triplinervis* morphotypes have a hepatotoxic effect. Further studies are needed.

The itching was an effect described in the hypocratic screening and may be related to irritation and sensitivity caused by the oxide and quinone groups of Caryophyllene oxide, 2,5-Di-*tert*-buthyl-1,4-benzenoquinone, and α-cedrene epoxide in the skin predicted by the analyses of DEREK. The presence of a skin sensitization structural alert within a molecule indicates the molecule has the potential to cause skin sensitization. Whether the molecule is a skin sensitizer will also depend upon its percutaneous absorption. Generally, small lipophilic molecules are more readily absorbed into the skin and are therefore more likely to cause sensitization (Basketter and Scholes, 1992).

Thus, it is possible to conclude that nano-emulsions have low acute dermal toxicity and indicated that the LD_{50} is higher than 2000 $mg.Kg^{-1}$ and can be used in the chemical control of *A. aegypti* adults.

5. Conclusions

Docking showed inhibition of the catalytic site of acetylcholinesterase enzyme receptors by acyphyllene, α-muurulene, γ-gurjunene, valencene, and α-cedrene epoxide, and inhibition of juvenile hormone receptors by α-muurulene, β-selinene, γ-gurjunene, and α-cedrene epoxide and indicated the insecticidal potential of *A. triplinervis* morphotypes *in silica* model.

The evaluation of adulticidal activity showed that the diagnostic dose of 150 $\mu g.mL^{-1}$ in the diagnostic time of 15 min for MAEON, and MBEON was the same diagnostic dose in 45 min of exposure. These results indicate the susceptibility of *A. aegypti* against *A. triplinervis* nano-emulsions. Nano-emulsions have low acute dermal toxicity and the LD_{50} is higher than 2000 $mg.Kg^{-1}$.

Declaration of Competing Interest

The authors declare that they have no known competing financial interests or personal relationships that could have appeared to influence the work reported in this paper.

Acknowledgments

The Amapá Research Support Foundation (FAPEAP). To the Research Program for SUS – PPSUS – Ministry of Health. The Coordination for the Improvement of Higher Education Personnel (CAPES)/Ministry of Education (MEC). To the Pharmaceutical Research laboratory – UNIFAP under the responsibility of Dr. José Carlos Tavares Carvalho. To the Laboratory of Toxicology and Pharmaceutical Chemistry – UNIFAP under the responsibility of Dr. Mayara Amoras Teles Fujishima. The Dean of Research and Graduate Studies – PROPESPG.

References

Aïzoun, N., Aïkpon, R., Azondekon, R., Gnanguenon, V., Osse, R., Padonou, G.G., Akogbéto, M., 2014. Centre for Disease Control and Prevention (CDC) bottle bioassay: A real complementary method to World Health Organization (WHO) susceptibility test for the determination of insecticide susceptibility in malaria vectors. J. Parasitol. Vector Biol. 6, 42–47.

Alomar, A.A., Eastmond, B.H., Alto, B.W., 2021. Juvenile hormone analog enhances Zika virus infection in Aedes aegypti. Sci. Rep. 11, 21062. https://doi.org/10.1038/s41598-021-00432-1.

Araj, S.-E.-A., Salem, N.M., Ghabeish, I.H., Awwad, A.M., 2015. Toxicity of Nanoparticles against *Drosophila melanogaster* (Diptera: Drosophilidae). J. Nanomaterials 2015. https://doi.org/10.1155/2015/758132.

Arung, E.T., Kuspradini, H., Kusuma, I.W., Shimizu, K., Kondo, R., 2012. Validation of Eupatorium triplinerve Vahl Leaves, a Skin Care Herb from East Kalimantan, Using a Melanin Biosynthesis Assay. J. Acupuncture Meridian Studies 5. https://doi.org/10.1016/j.jams.2012.01.003.

Basketter, D.A., Scholes, E.W., 1992. Comparison of the local lymph node assay with the guinea-pig maximization test for the detection of a range of contact allergens. Food Chem. Toxicol. 30. https://doi.org/10.1016/0278-6915(92)90138-B.

Bhavya, M.L., Chandu, A.G.S., Devi, S.S., 2018. Ocimum tenuiflorum oil, a potential insecticide against rice weevil with anti-acetylcholinesterase activity. Ind. Crops Prod. 126. https://doi.org/10.1016/j.indcrop.2018.10.043.

Bose, O., Gupta, M., Kanti Mazumder, U., Sambath Kumar, R., Sivakumar, H., Suresh Kumar, R., 2007. Hepatoprotective and Antioxidant Effects of Eupatorium ayapana against Carbon Tetrachloride nduced Hepatotoxicity in Rats. J. Pharmacol. Therapeut.

Brandão, L.B., Santos, L.L., Martins, R.L., Rodrigues, A.B.L., Rabelo, E. de M., Galardo, A.K.R., Almeida, S.S.M. da S. de, 2021. Larvicidal Evaluation against Aedes aegypti and Antioxidant and Cytotoxic Potential of the Essential Oil of Tridax procumbens L. Leaves. The Scientific World Journal 2021. https://doi.org/10.1155/2021/2172919.

Brogdon, W.G., Chan, A., 2013. Diretriz para Avaliar a Resistência a Inseticida em Vetores Usando o Bioensaio com Garrafa do CDC, 1st ed.

Calleja, M.A., Vieites, J.M., Montero-Meterdez, T., Torres, M.I., Faus, M.J., Gil, A., Suárez, A., 2013. The antioxidant effect of β-caryophyllene protects rat liver from carbon tetrachloride-induced fibrosis by inhibiting hepatic stellate cell activation. Br. J. Nutr. 109. https://doi.org/10.1017/S0007114512001298.

Castillo, R.M., Stashenko, E., Duque, J.E., 2017. Insecticidal and Repellent Activity of Several Plant-Derived Essential Oils Against *Aedes aegypti*. J Am Mosq Control Assoc 33. https://doi.org/10.2987/16-6585.1.

Chaves, R. do S.B., Martins, R.L., Rodrigues, A.B.L., Rabelo, É. de M., Farias, A.L.F., Brandão, L.B., Santos, L.L., Galardo, A.K.R., de Almeida, S.S.M. da S., 2020. Evaluation of larvicidal potential against larvae of Aedes aegypti (Linnaeus, 1762) and of the antimicrobial activity of essential oil obtained from the leaves of Origanum majorana L. PLOS ONE 15. https://doi.org/10.1371/journal.pone.0235740.

Chokechaijaroenporn, O., Bunyapraphatsara, N., Kongchuensin, S., 1994. Mosquito repellent activities of ocimum volatile oils. Phytomedicine 1. https://doi.org/10.1016/S0944-7113(11)80031-0.

Consoli, R., Oliveira, R., 1994. Principais Mosquitos de Importância Sanitária no Brasil. Editora Fiocruz, Rio de Janeiro.

Costa, G., Ferreira, E.F.B., da S. Ramos, R., B. da Silva, L., M. F. de Sá, E., K. P. da Silva, A., M. Lobato, C., N. P. Souto, R., T. de P. da Silva, C.H., B. Federico, L., M. C. Rosa, J., B. R. dos Santos, C., 2019a. Hierarchical Virtual Screening of Potential Insectides Inhibitors of Acetylcholinesterase and Juvenile Hormone from Temephos. Pharmaceuticals 12. https://doi.org/10.3390/ph12020061.

Crawford, J.E., Alves, J.M., Palmer, W.J., Day, J.P., Sylla, M., Ramasamy, R., Surendran, S.N., Black, W.C., Pain, A., Jiggins, F. M., 2017. Population genomics reveals that an anthropophilic population of Aedes aegypti mosquitoes in West Africa recently gave rise to American and Asian populations of this major disease vector. BMC Biol. 15. https://doi.org/10.1186/s12915-017-0351-0.

Croom, E., 2012. Metabolism of Xenobiotics of Human Environments. In: Hodgson, E. (Ed.), Progress in Molecular Biology and Translational Science. Academic Press, Oxford. https://doi.org/10.1016/B978-0-12-415813-9.00003-9.

Cusson, M., Sen, S.E., Shinoda, T., 2013. Juvenile Hormone Biosynthetic Enzymes as Targets for Insecticide Discovery, in: Ishaaya, I., Palli, S., Horowitz, A.R. (Eds.), Advanced Technologies for Managing Insect Pests. Springer Netherlands, Dordrecht. https://doi.org/10.1007/978-94-007-4497-4_3.

Drwal, M.N., Banerjee, P., Dunkel, M., Wettig, M.R., Preissner, R., 2014. ProTox: a web server for the in silico prediction of rodent oral toxicity. Nucleic Acids Res. 42. https://doi.org/10.1093/nar/gku401.

Durán, N., Islan, G.A., Durán, M., Castro, G.R., 2016. Nanobiotechnology Solutions against *Aedes aegypti*. J. Braz. Chem. Soc. https://doi.org/10.5935/0103-5053.20160122.

Gauvin-Bialecki, A., Marodon, C., 2008. Essential oil of Ayapana triplinervis from Reunion Island: A good natural source of thymohydroquinone dimethyl ether. Biochem. Syst. Ecol. 36. https://doi.org/10.1016/j.bse.2008.09.006.

Ghattas, M.A., al Rawashdeh, S., Atatreh, N., Bryce, R.A., 2020. How Do Small Molecule Aggregates Inhibit Enzyme Activity? A Molecular Dynamics Study. Journal of Chemical Information and Modeling 60, 3901–3909. https://doi.org/10.1021/acs.jcim.0c00540.

Guerra-Rosas, M.I., Morales-Castro, J., Ochoa-Martínez, L.A., Salvia-Trujillo, L., Martín-Belloso, O., 2016. Long-term stability of food-grade nano-emulsions from high methoxyl pectin containing essential oils. Food Hydrocolloids 52. https://doi.org/10.1016/j.foodhyd.2015.07.017.

Gupta, R.C., Doss, R.B., Srivastava, A., Lall, R., Sinha, A., 2019. Nutraceuticals for Control of Ticks, Fleas, and Other Ectoparasites, in: Gupta, R., Srivastava, A., Lall, R. (Eds.), Nutraceuticals in Veterinary Medicine. Springer International Publishing, Cham. https://doi.org/10.1007/978-3-030-04624-8_43.

Gustafsson, M.H.G., Bremer, K., 1995. Morphology and phylogenetic interrelationships of the Asteraceae, Calyceraceae, Campanulaceae, Goodeniaceae, and related families (Asterales). Am. J. Bot. 82. https://doi.org/10.1002/j.1537-2197.1995.tb11493.x.

Haddi, K., Tomé, H.V.V., Du, Y., Valbon, W.R., Nomura, Y., Martins, G.F., Dong, K., Oliveira, E.E., 2017. Detection of a new pyrethroid resistance mutation (V410L) in the sodium channel of Aedes aegypti: a potential challenge for mosquito control. Sci. Rep. 7. https://doi.org/10.1038/srep46549.

Harel, M., Kryger, G., Rosenberry, T.L., Mallender, W.D., Lewis, T., Fletcher, R.J., Guss, J.M., Silman, I., Sussman, J.L., 2000. Three-dimensional structures of *Drosophila melanogaster* acetylcholinesterase and of its complexes with two potent inhibitors. Protein Sci. 9. https://doi.org/10.1110/ps.9.6.1063.

Khanikor, B., 2013. Comparative mode of action of some terpene compounds against octopamine receptor and acetyl cholinesterase of mosquito and human system by the help of homology modeling and Docking studies. J. Appl. Pharm. Sci. https://doi.org/10.7324/JAPS.2013.30202.

Kim, I.H., Pham, V., Jablonka, W., Goodman, W.G., Ribeiro, J.M.C., Andersen, J.F., 2017. A mosquito hemolymph odorant-binding protein family member specifically binds juvenile hormone. J. Biol. Chem. 292. https://doi.org/10.1074/jbc.M117.802009.

Kliewer, S.A., Goodwin, B., Willson, T.M., 2002. The Nuclear Pregnane X Receptor: A Key Regulator of Xenobiotic Metabolism. Endocr. Rev. 23. https://doi.org/10.1210/er.2001-0038.

Lee, S.-H., Ha, K.B., Park, D.H., Fang, Y., Kim, J.H., Park, M.G., Woo, R.M., Kim, W.J., Park, I.-K., Choi, J.Y., Je, Y.H., 2018. Plant-derived compounds regulate formation of the insect juvenile hormone receptor complex. Pestic. Biochem. Physiol. 150. https://doi.org/10.1016/j.pestbp.2018.06.013.

López, M.D., Pascual-Villalobos, M.J., 2010. Mode of inhibition of acetylcholinesterase by monoterpenoids and implications for pest control. Ind. Crops Prod. 31. https://doi.org/10.1016/j.indcrop.2009.11.005.

Melo, A.S., Monteiro, M.C., da Silva, J.B., de Oliveira, F.R., Vieira, J. L.F., de Andrade, M.A., Baetas, A.C., Sakai, J.T., Ferreira, F.A., Cunha Sousa, P.J. da, Maia, C. do S.F., 2013. Antinociceptive, neurobehavioral and antioxidant effects of Eupatorium triplinerve Vahl on rats. J. Ethnopharmacol. 147. https://doi.org/10.1016/j.jep.2013.03.002.

Moralev, S.N., Rozengart, E.V., Suvorov, A.A., 2001. The "Catalytic Machines" of Cholinesterases of Different Animals Have the Same Structure. Doklady Biochem. Biophys. 381. https://doi.org/10.1023/A:1013351127011.

Nenaah, G.E., Ibrahim, S.I.A., Al-Assiuty, B.A., 2015. Chemical composition, insecticidal activity and persistence of three Asteraceae essential oils and their nano-emulsions against Callosobruchus maculatus (F.). J. Stored Prod. Res. 61. https://doi.org/10.1016/j.jspr.2014.12.007.

Nery, M.I.S., Potiguara, R.C.V., Kikuchi, T.Y.S., Garcia, T.B., Lins, A.L.F.A., 2014. Morfoanatomia do eixo vegetativo aéreo de Ayapana triplinervis (Vahl) R.M. King & H. Rob. (Asteraceae). Revista Brasileira de Plantas Medicinais 16. https://doi.org/10.1590/S1516-05722014000100009.

Oboh, G., Ademosun, A.O., Olumuyiwa, T.A., Olasehinde, T.A., Ademiluyi, A.O., Adeyemo, A.C., 2017. Insecticidal activity of essential oil from orange peels (Citrus sinensis) against Tribolium confusum, Callosobruchus maculatus and Sitophilus oryzae and its inhibitory effects on acetylcholinesterase and Na+/K+-ATPase activities. Phytoparasitica 45. https://doi.org/10.1007/s12600-017-0620-z.

Oecd, 2017. Test No. 402: Acute Dermal Toxicity. OECD. https://doi.org/10.1787/9789264070585-en.

Park, C.G., Jang, M., Yoon, K.A., Kim, J., 2016. Insecticidal and acetylcholinesterase inhibitory activities of Lamiaceae plant essential oils and their major components against Drosophila suzukii (Diptera: Drosophilidae). Ind. Crops Prod. 89. https://doi.org/10.1016/j.indcrop.2016.06.008.

Rai, V.K., Mishra, N., Yadav, K.S., Yadav, N.P., 2018. Nanoemulsion as pharmaceutical carrier for dermal and transdermal drug delivery: Formulation development, stability issues, basic considerations and applications. J. Control. Release 270. https://doi.org/10.1016/j.jconrel.2017.11.049.

Ramos, R.S., Macêdo, W.J.C., Costa, J.S., da Silva, C.H.T. de P., Rosa, J.M.C., da Cruz, J.N., de Oliveira, M.S., de Aguiar Andrade, E.H., e Silva, R.B.L., Souto, R.N.P., Santos, C.B.R., 2020a. Potential inhibitors of the enzyme acetylcholinesterase and juvenile hormone with insecticidal activity: study of the binding mode via docking and molecular dynamics simulations. J. Biomol. Struct. Dyn. 38. https://doi.org/10.1080/07391102.2019.1688192.

Ridings, J.E., Barratt, M.D., Cary, R., Earnshaw, C.G., Eggington, C. E., Ellis, M.K., Judson, P.N., Langowski, J.J., Marchant, C.A., Payne, M.P., Watson, W.P., Yih, T.D., 1996. Computer prediction of possible toxic action from chemical structure: an update on the DEREK system. Toxicology 106. https://doi.org/10.1016/0300-483X(95)03190-Q.

Rodrigues, A.B., Martins, R.L., Rabelo, É. de M., Tomazi, R., Santos, L.L., Brandão, L.B., Faustino, C.G., Ferreira Farias, A.L., Santos, C.B.R., Castro Cantuária, P., Galardo, A.K.R., Almeida, S.S.M. da S., 2021. Development of nano-emulsions based on Ayapana triplinervis essential oil for the control of Aedes aegypti larvae. PLOS ONE 16, e0254225. https://doi.org/10.1371/journal.pone.0254225.

Rückert, C., Weger-Lucarelli, J., Garcia-Luna, S.M., Young, M.C., Byas, A.D., Murrieta, R.A., Fauver, J.R., Ebel, G.D., 2017. Impact of simultaneous exposure to arboviruses on infection and transmission by Aedes aegypti mosquitoes. Nat. Commun. 8. https://doi.org/10.1038/ncomms15412.

Rudik, A. v., Dmitriev, A. v., Lagunin, A.A., Filimonov, D.A., Poroikov, V.V., 2016. Prediction of reacting atoms for the major biotransformation reactions of organic xenobiotics. Journal of Cheminformatics 8. https://doi.org/10.1186/s13321-016-0183-x.

Rudik, A. v., Bezhentsev, V.M., Dmitriev, A.V., Druzhilovskiy, D.S., Lagunin, A.A., Filimonov, D.A., Poroikov, V.V., 2017. MetaTox: Web Application for Predicting Structure and Toxicity of Xenobiotics' Metabolites. Journal of Chemical Information and Modeling 57. https://doi.org/10.1021/acs.jcim.6b00662.

Santos, C.B.R., da Silva Ramos, R., Ortiz, B.L.S., da Silva, G.M., Giuliatti, S., Balderas-Lopez, J.L., Navarrete, A., Carvalho, J.C.T., 2018. Oil from the fruits of Pterodon emarginatus Vog.: A traditional anti-inflammatory. Study combining in vivo and in silico. J. Ethnopharmacol. 222. https://doi.org/10.1016/j.jep.2018.04.041.

Selvamangai, G., Bhaskar, A., 2012. GC–MS analysis of phytocomponents in the methanolic extract of Eupatorium triplinerve. Asian Pacific J. Tropical Biomed. 2. https://doi.org/10.1016/S2221-1691(12)60410-9.

Seo, S.-M., Jung, C.-S., Kang, J., Lee, H.-R., Kim, S.-W., Hyun, J., Park, I.-K., 2015. Larvicidal and Acetylcholinesterase Inhibitory Activities of Apiaceae Plant Essential Oils and Their Constituents against *Aedes albopictus* and Formulation Development. J. Agric. Food. Chem. 63. https://doi.org/10.1021/acs.jafc.5b03586.

Silva, N.N.S., Silva, J.R.A., Alves, C.N., Andrade, E.H.A., da Silva, J. K.R., Maia, J.G.S., 2014. Acetylcholinesterase Inhibitory Activity and Molecular Docking Study of 1-Nitro-2-Phenylethane, the Main Constituent of *Aniba canelilla* Essential Oil. Chem. Biol. Drug Des. 84. https://doi.org/10.1111/cbdd.12304.

Vázquez, J., López, M., Gibert, E., Herrero, E., Luque, F.J., 2020. Merging Ligand-Based and Structure-Based Methods in Drug Discovery: An Overview of Combined Virtual Screening Approaches. Molecules 25, 4723–4750. https://doi.org/10.3390/molecules25204723.

Veerakumar, K., Govindarajan, M., Hoti, S.L., 2014. Evaluation of plant-mediated synthesized silver nanoparticles against vector mosquitoes. Parasitol. Res. 113. https://doi.org/10.1007/s00436-014-4147-7.

World Health Organization, 2016. Test procedures for insecticide resistance monitoring in malaria vector mosquitoes. WHO Press, Switzerland.

Wu, J., Liu, H., Ge, S., Wang, S., Qin, Z., Chen, L., Zheng, Q., Liu, Q., Zhang, Q., 2015. The preparation, characterization, antimicrobial stability and in vitro release evaluation of fish gelatin films incorporated with cinnamon essential oil nanoliposomes. Food Hydrocolloids 43. https://doi.org/10.1016/j.foodhyd.2014.06.017.